

Research Submission

Diffusion Tensor Imaging in Episodic Cluster Headache

Michael Teepker, MD; Katja Menzler, MD; Marcus Belke, MD; Johannes T. Heverhagen, MD;
Maximilian Voelker, BA; Veit Mylius, MD; Wolfgang H. Oertel, MD; Felix Rosenow, MD;
Susanne Knake, MD

Background.—Cluster headache (CH) is a rare headache disorder with severe unilateral headache bouts and autonomic symptoms. The pathophysiology of CH is not completely understood. Using a voxel-based morphometric paradigm or functional imaging, a key role of the hypothalamus and the pain matrix could be demonstrated during CH episodes. However, there are no diffusion tensor imaging (DTI) data investigating the white matter microstructure of the brain in patients with CH. Therefore, we used DTI to delineate microstructural changes in patients with CH in a headache-free state.

Methods.—Seven male patients with episodic CH and 7 healthy subjects were included and examined with a routine 1.5 T magnetic resonance imaging scanner. Whole-head DTI scans measuring fractional anisotropy were analyzed without a priori hypotheses using track-based spatial statistics.

Results.—We found significant microstructural brain tissue changes bilaterally in the white matter of the brainstem, the frontal lobe, the temporal lobe, the occipital lobe, the internal capsule, and on the right side of thalamus and cerebellum. There were further lesions in the basal frontal lobe that were part of the olfactory system. Alterations of fractional anisotropy in the brainstem might indicate changes of the medial lemniscus and central sympathetic pathways.

Conclusions.—Patients with episodic CH have microstructural brain changes in regions that belong to the pain matrix. Furthermore, we were able to detect structural changes suggesting an involvement of the olfactory system as well as lesions in the brainstem indicating an involvement of trigeminal and sympathetic systems.

Key words: DTI, MRI, episodic cluster headache, white matter lesions, headache, pain matrix

(*Headache* 2012;52:274-282)

Cluster headache (CH) is a rare primary headache disease clinically impressing with severe unilateral headache attacks and ipsilateral parasympathetic (eg, lacrimation or rhinorrhea) or sympathetic (eg, miosis or ptosis) symptoms that occur in periodical bouts and mainly affect men.¹ Episodic CH, the most common

form, is defined as cluster periods with complete remission for at least 1 month.¹⁻³ The circadian and clock-like appearing clinical features suggest that the hypothalamus as the “biological clock” plays a key role in the pathophysiology of CH. In fact, neuroimaging techniques using positron emission tomography (PET)^{4,5} or functional magnetic resonance imaging (fMRI)⁶ could demonstrate an activation of the hypothalamus during attacks of CH. Using those functional imaging techniques, areas of the pain matrix, such as the anterior cingulate cortex (ACC), the contralateral posterior thalamus, the ipsilateral basal ganglia, the bilateral insulae, and the cerebellar hemispheres, were activated, too.^{5,7} In spite of these findings, the pathophysiology of CH is still not completely understood.

From the Department of Neurology, Philipps-University of Marburg, Marburg, Germany (M. Teepker, K. Menzler, M. Belke, V. Mylius, W.H. Oertel, F. Rosenow, S. Knake); Department of Diagnostic Radiology, Philipps-University of Marburg, Marburg, Germany (J.T. Heverhagen, M. Voelker).

Address all correspondence to S. Knake, Department of Neurology, Section of Brain Imaging, Baldingerstr., 35033 Marburg, Germany, email: knake@staff.uni-marburg.de

Accepted for publication June 6, 2011.

Conflict of Interest: No conflicts.

One study analyzed gray matter changes in patients with CH using a voxel-based morphometric (VBM) analysis. The authors found differences in gray matter density bilaterally in the diencephalon. The authors suggested a structural correlate of CH.⁵ Diffusion tensor imaging (DTI) is a novel MRI technique that enables the visualization of microstructural alteration of white matter brain structure non-invasively. Using DTI, microstructural brain changes of several other neurologic disorders⁸⁻¹¹ have been shown.

We used whole head DTI in patients with episodic CH to delineate microstructural brain changes and to further investigate the underlying pathophysiology of CH.

METHODS

Subjects.—Seven male patients suffering from episodic CH at the age of 29-68 years (mean age = 43.14 ± 13.42 years) were included. Three subjects described right-sided attacks, 4 had left-sided ones. The duration of the CH disease ranged from 2 years to 20 years. At study time only 1 patient suffered from active CH bouts since 5 days. Further detailed characteristics such accompanying diseases are demonstrated in Table 1. Seven healthy male controls (mean age = 50.43 ± 7.89 years) were included and matched for age (ANOVA for age differences between groups: $F(1/12) = 1.53$; $P = .24$).

Subjects were recruited from the outpatient clinic of the Neurological Department, University of Marburg. For inclusion, subjects had to suffer from CH according to the guidelines of the International Headache Society.² Exclusion criteria for all participants were: contraindication for an MRI and a history of other psychiatric or neurological diseases, especially no history of headache or pain diseases occurring regularly or chronically. Before inclusion, patients were examined by a headache-specialized neurologist.

The study protocol was reviewed and approved by the local internal review board. All enrolled subjects provided written informed consent to participate in this study.

MRI Acquisition.—Microstructural brain tissue integrity was assessed using DTI measures of fractional anisotropy (FA). The DTI scans were collected on a Siemens 1.5 T Sonata MRI scanner (Siemens

Medical Solutions, Erlangen, Germany), using a cp head array coil. A single-shot echo planar sequence with a twice-refocused spin echo pulse, optimized to minimize eddy current-induced image distortions was performed with the following parameters: TR/TE = 10600/104 ms, TI = -1 ms, Flip Angle = 90°, $b = 1000 \text{ s/mm}^2$, $256 \times 256 \text{ mm FOW}$, $128 \times 128 \times 60$ matrix, voxel size $2 \times 2 \times 2.4 \text{ mm}$. Five T2 b0 images with a b value of 0 and otherwise with exactly the same parameters as the diffusion weighted images, and 30 diffusion weighted imaging (DWI) b1000 images were collected during 1 scan. The 5 b0 images were collected first, followed by the 30 DWI images. A mean low- b image was calculated using all 5 b0 weighted scans.

To minimize motion artifacts the head of the subject was firmly fixed in the head coil. All images were investigated to be free of motion or ghosting, high frequency and/or wrap-around artifacts at the time of image acquisition. The T2 b0 images were analyzed to determine whether changes other than those in tissue microstructure contributed to the observed effects, such as technical artifacts or individual large-scale signal changes such as white matter signal abnormalities (eg, hyperintensities).

DTI Preprocessing and Analysis.—Image preprocessing was performed as described previously:^{2,10} diffusion volumes were motion-corrected and averaged using FLIRT (Oxford Centre for Functional MRI of the Brain [FMRIB's] Linear Image Registration Tool; <http://www.fmrib.ox.ac.uk/analysis/research/flirt/>)¹² with mutual information cost function to register each direction to the minimally eddy current distorted T2-weighted b0 DTI volume that had no diffusion weighting.

Eigenvalues ($\lambda_1, \lambda_2, \lambda_3$) and eigenvectors of the diffusion tensor matrix for each voxel were computed from the DTI volumes for each subject on a voxel-by-voxel basis using conventional reconstruction methods.^{13,14} The tools are included in the FreeSurfer package (FreeSurfer version 4.2.0; <http://surfer.nmr.mgh.harvard.edu/>).

FA Map Calculation.—The primary measure acquired from the DTI data was the FA, a scalar metric unit describing the white matter microstructure. FA was calculated using the standard formula defined previously.^{10,13}

Table 1.—Basic Clinical Characteristics of the Patients Suffering From CH Included Into This Study

	Age	Site of CH	Duration of CH disease (years)	Duration of CH attacks in a cluster period	Frequency of CH attacks during a cluster period	Number of CH bouts during the last 5 years	Cluster period at the moment?	Prophylactic medication at the moment?	Accompanying diseases	A further accompanying medication
#1	35	Left	10	1 hour	2 per day	5	Yes, since 5 days	Verapamil	None	None
#2	68	Left	13	1 hour	3 per day	2	No	None	Benign tumor of the thyroid gland	Levothyroxine
#3	36	Right	4	Up to 3 hours	3 per day	3	No	Verapamil	IDDM, asthma bronchiale	Insulin
#4	42	Left	12	0.5-1 hour	3-4 per day	3	No	None	None	None
#5	38	Left	20	3 hours	Up to 8 per day	8	No	Lithium extended release	None	None
#6	54	Right	2	30-50 minutes	1 per day	2	No	None	NIDDM, polyneuropathy	None
#7	29	Right	10	45 minutes to 3 hours	1 per day	3	No	Verapamil	None	None

The respective characteristics include age, site of CH attacks, duration of CH, duration and frequency of CH attacks during active bouts, number of CH bouts during the last 5 years, active bouts or prophylactic medications at the moment and accompanying diseases with further medications. All subjects were male and suffered from episodic cluster headache.

CH = cluster headache; IDDM = insulin-dependent diabetes mellitus; NIDDM = non-insulin-dependent diabetes mellitus.

Nonlinear Registration and Tract-Based Spatial Statistics.—Voxelwise statistical analysis of the FA data was carried out using Tract-Based Spatial Statistics (TBSS),¹⁵ which is part of the FSL data analysis suite (FSL 4.1.2; <http://www.fmrib.ox.ac.uk/fsl/>).¹⁶ First, the T2 b0 images were brain-extracted using the BET-tool of the FSL stream. Those extracted brains were used to mask the FA images. The common space was given by the automatically selected subject, which was most representative for the whole group. All subjects' masked FA data were then aligned into this common space using the nonlinear registration tool FNIRT,¹⁷ which uses a b-spline representation of the registration warp field.¹⁸ Last, all subjects were finely registered to voxel spaces of the MNI152 brain. Next, a mean FA image was created and thinned to create a mean FA skeleton, which represents the centers of all tracts the group has in common. A threshold of $FA > 0.2$ was applied to the skeleton to include only major fiber bundles. Each subject's aligned FA data was then projected onto this skeleton. Data along the skeleton were smoothed utilizing an anatomical constraint to limit the smoothing to neighboring data within adjacent voxels along the skeleton. For smoothing, the neighboring voxels within a cube of 6 mm edge length were used to calculate the mean. The smoothing step was performed using Matlab (Matlab 7.6.0.324, MathWorks, Aachen, Germany). All analyses were masked to only display regions with FA values of >0.2 as an additional procedure to avoid examination of regions that are likely composed of multiple tissue types or fiber orientations.

Brain Flipping.—To virtually create a population having the symptoms on the same side, the brains of patients with complaints on the right side were flipped in the x -axis. After this step, all patients had the symptomatic side left side and an asymptomatic side on the right side. We used the tool *fslswapdim* of the FSL package to calculate this step. Afterwards these flipped images were analyzed in exactly the same way as described before.

Group Analysis.—The skeletonized images were used for voxelwise cross-subject statistics. The group analysis was calculated with the *mriglmsfit* tool of the FreeSurfer stream fitting data into a generalized linear model and performing an unpaired t -test. The

resulting data were corrected for multiple comparisons by a permutation-based approach.¹⁹ 12,000 simulations were performed under the null hypothesis; this approach was based on the AFNI null-z simulator (*AlphaSim*; <http://afni.nimh.nih.gov/afni/doc/manual/AlphaSim>). Last, the data were clustered; in this step several connected voxels were searched and merged into 1 cluster. For the clustering we only considered voxels with a minimum significance of $P < .01$. To display the results, all figures were made with exactly the same parameters, showing clusters with a significance of $P < .01$, all regions were dilated for better visualization, using the *dilM* function of the FSL tool *fslmaths*. The correction for multiple testing was performed for the clusters with the *mri_glmfit-sim* tool of the FreeSurfer package. Results were summarized in Table 2 showing the localization of the clusters and their significances.

RESULTS

We found significant regional changes of FA (corrected $P < .0001$) in the brain stem, the thalamus, the internal capsule, the superior and inferior temporal region, the frontal lobe, the occipital lobe and the cerebellum. The results are demonstrated in Table 2 and in the Figure.

DISCUSSION

We report regional microstructural brain changes in patients with CH. Using DTI, we found morphological changes in different white matter brain regions such as the brainstem, frontal, temporal, and occipital areas as well as the internal capsule and in the right cerebellum and thalamus.

Up to now, only limited data exist on structural, functional, and metabolic changes during the cluster episodes, suggesting neural correlates of the disease in the ipsilateral hypothalamus, the contralateral ventroposterior thalamus, the ACC, the insula bilaterally, the cerebellar hemispheres bilaterally, as well as the vermis.⁴ Whereas the hypothalamic involvement is thought to be specific for CH and might explain its circadian rhythmicity, the other regions are generally activated in pain processing and contribute to a pain regulating network ("pain matrix"). Because of methodological constraints, the hypo-

Table 2.—Regions With Clusters of Significant Fractional Anisotropy Changes

Region	Size (mm ³)	Maximum <i>P</i> (10 ^{-x})	Corrected Overall <i>P</i>	X	Y	Z
Brain stem						
Right	144	3.11	<0.0001	80	100	53
Left	186	3.47	<0.0001	99	104	61
Middle	26	2.21	<0.0001	89	93	48
Temporal region (superior)						
Right	149	3.81	<0.0001	31	105	79
Left	154	5.39	<0.0001	148	109	61
Cerebellum						
Right	362	3.19	<0.0001	49	67	30
Vermis	27	2.04	<0.0001	89	62	35
Frontal region						
Right	282	2.93	<0.0001	68	157	69
Left	193	4.63	<0.0001	110	159	68
Olfactory	256	2.66	<0.0001	77	173	48
Temporal region (inferior)						
Right	170	4.43	<0.0001	35	127	38
Left	448	4.2	<0.0001	135	120	40
Thalamus						
Right	53	2.62	<0.0001	86	118	82
Internal capsule						
Right anterior	54	2.76	<0.0001	70	138	78
Right posterior	77	2.13	<0.0001	76	121	71
Left anterior	88	3.19	<0.0001	107	136	65
Occipital						
Right	122	5.04	<0.0001	49	47	73
Left	298	3.3	<0.0001	126	49	70
Precuneus	201	3.8	<0.0001	102	60	111

X, Y, Z are the corresponding voxel spaces of the MNI152 brain. Cluster size is given in mm³. The z values represent the axial position of the MNI coordinates.

thalamus was not included in our analysis. Using TBSS to control for method-inherent shortcomings, such as registration and spatial smoothing errors, we excluded smaller brain regions with high interindividual anatomical variability like the hypothalamus from the analysis. However, in the light of the current literature,^{4,5} there is no doubt about the key role of the hypothalamus in the pathophysiology of CH. In fact, treatment of CH is possible by high-frequency stimulation of the hypothalamus (for review see Leone and Bussone²⁰).

A recent study could demonstrate an altered glucose metabolism in frontal brain circuits in CH using ¹⁸F-fluoro-2-deoxy-D-glucose-positron emission tomography (FDG-PET).²¹ An increase of metabolism during cluster attacks could be observed in the perigenual ACC, posterior cingulate cortex, prefrontal cortex, insulae, thalamus and temporal cortex. In contrast to healthy volunteers, CH patients

revealed hypometabolism in the perigenual ACC, prefrontal and orbito-frontal cortex. Regarding the activation of frontal brain regions during CH attacks, the authors claimed a role in supraspinal pain processing by modulating descending pain inhibitory circuits.^{22,23} The impairment of frontal pain modulating systems is considered to make patients more susceptible to the generation of pain. In this study, we could observe distinct FA alterations in the frontal lobe, the right thalamus and in the anterior limb of the internal capsule bilaterally containing thalamo-frontal projections. These findings underline the theory of disturbances of thalamo-frontal circuits in CH making patients more susceptible to pain.²¹ Interestingly, lesions were found in orbito-frontal regions that might contribute to the olfactory system.

Others hypothesize that structures of the pain matrix are active during cluster attacks including subcortical structures such as amygdala for emotional or

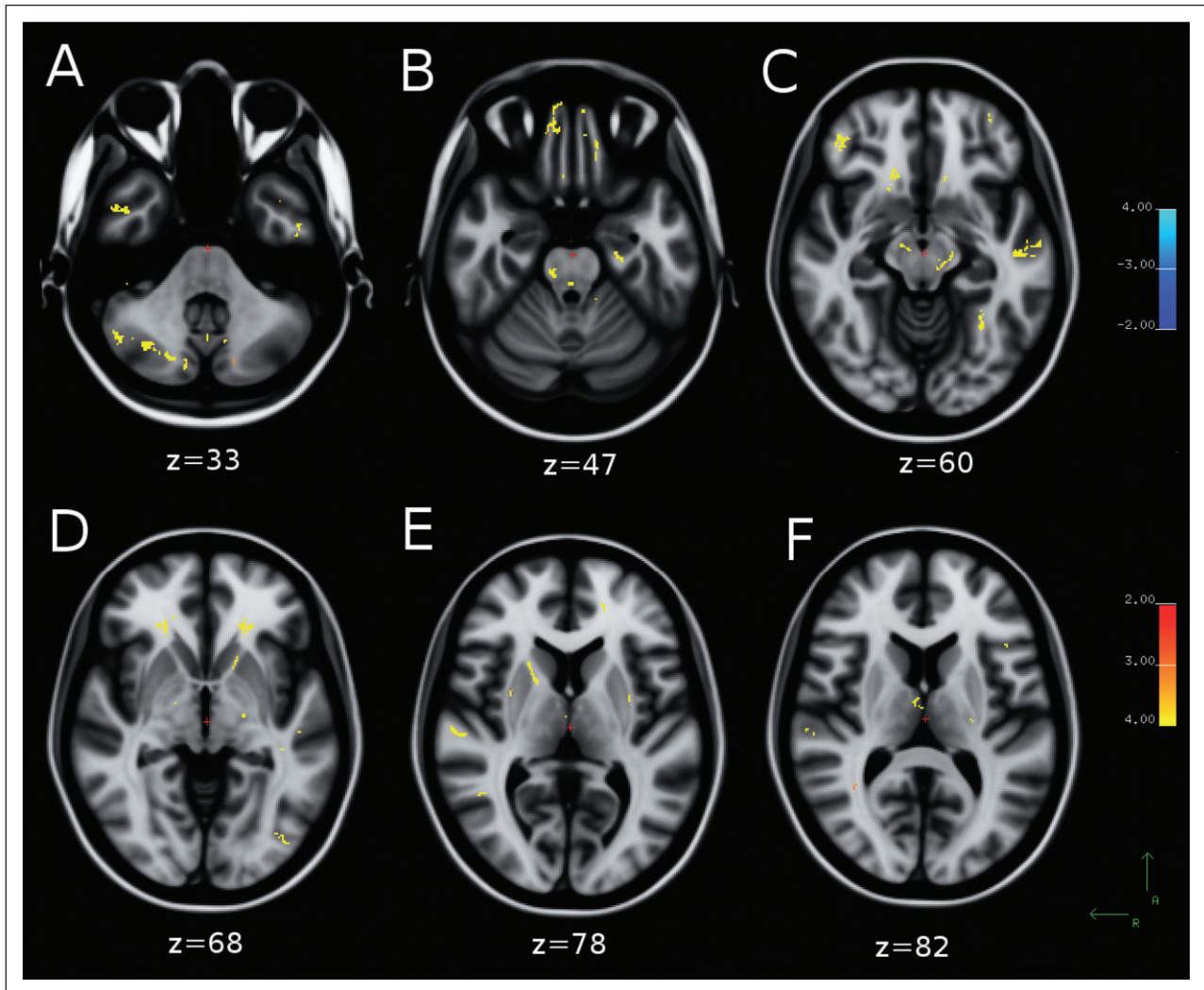


Figure.—Changes of fractional anisotropy in patients suffering from episodic cluster headache suggesting altered white matter microstructure. The yellow spots indicate significance ($P < .0001$) when compared with healthy volunteers. (A) Microstructural brain changes in the corresponding areas of the right cerebellar hemisphere, vermis and bitemporally. (B) Structural changes in the brainstem, in the left parahippocampal and in the fronto-polar region bilaterally (right > left). (C) Microstructural white matter changes in frontal as well as temporal brain regions. The lesions in the upper brainstem might indicate an involvement of the nucleus tractus spinalis n. trigemini and the central sympathetic pathway. (D) White matter lesions in the anterior limb of the left internal capsule and bifrontally. (E) White matter lesions in the anterior limb of the right internal capsule. (F) White matter lesions in the right thalamus. The z values represent the axial position of the MNI coordinates.

affective actions,²⁴ hippocampus for memory and learning,²⁵ thalamus for arousal and attention,²⁶ as well as basal ganglia and cerebellum for motor function.²⁷ Whereas these parts of the motor systems respond asymmetrically, structures responsible for affective processes are activated symmetrically.²⁸

All those areas showed microstructural changes in our study, supporting the hypothesis that the pain matrix is structurally altered in patients with CH.

Further structural changes occurred in the posterior limb of the right internal capsule. These structures are part of the motor system and do not modulate nociceptive input but generate motor response to pain in terms of avoiding or defensive reactions.²⁸ The FA changes in the brainstem might indicate an involvement of the right medial lemniscus and the nucleus tractus trigemini affecting the trigemino-sensory system. The pain of CH is mediated via an

activation of the first trigeminal branch.²⁹ Lesions of the trigemino-sensory system are known to be associated with neuropathic facial pain.³⁰⁻³² Additionally, the left-sided FA changes of the upper brainstem might correspond to lesions of the central sympathetic pathway. The central sympathetic pathway projects to the hypothalamus. By this, we might have demonstrated lesions in the sympathetic and trigeminal systems in the brainstem that are crucially involved in the pathophysiology of CH.¹

Metabolic changes in the temporal lobe in CH were shown by Sprenger et al²¹ and parahippocampal regions are claimed to mediate antinociception or anxiolysis.³³ We found FA changes in temporal brain regions that occurred bilaterally and included parahippocampal structures on the left side. Further FA changes were evident bilaterally in posterior areas and in the left precuneus that responsible for episodic memory as described by Sprenger et al by PET.²¹ FA may assess microstructural brain tissue integrity. FA reflects the anisotropy or directionality of the diffusion and is an unspecific indicator of alterations in white matter microstructure,³⁴ which can be associated with changes in myelination or glial cell morphology³⁵⁻⁴⁰ or with changes in extra-axonal/extracellular space.^{39,40} However, a histopathological correlation is highly speculative.

One study using VBM found regional changes in gray matter density in the diencephalon bilaterally in a large cohort of CH patients.⁵ In contrast to this study, we were studying the integrity of large white matter bundles using DTI. Despite methodological differences and a much smaller study sample, our study confirmed microstructural differences in the upper brainstem of CH patients and revealed further microstructural lesion in brain regions that belong to the pain matrix. However, it is still unclear whether the observed structural changes are the primary etiology or a secondary phenomenon of the functionally altered pain matrix and to our knowledge no study has been able to answer this question so far. Interestingly, Schmitz et al⁴¹ could demonstrate in a cross-sectional study that brain abnormalities of the white matter (computing FA by DTI) and gray matter (using VBM) increase with attack frequency and disease duration in migraineurs. They concluded a

relationship between clinical features and microstructural abnormalities. Therefore, one can speculate that our findings in terms of white matter lesions might be—at least in some extent—caused by cluster attacks. In contrast to studies using functional and metabolic neuroimaging techniques such PET or fMRI, we could not demonstrate changes in the insula, ACC or dorsolateral, prefrontal cortex representing important parts of the pain matrix, which might be due to methodological differences.

There are some limitations to our study. As CH is a rare disorder mainly affecting men we were unfortunately only able to recruit 7 male patients. All patients included in our study suffered from episodic CH. Further, all participants differed clinically, eg, with respect to actual bouts, side of bouts, further diseases or actual medication. Because of these limitations, a correlation of clinical parameters with DTI findings was not possible.

We used TBSS, a novel registration approach that has advantages over conventional VBM-like analysis of DTI data are restricted to the analysis of the main white matter tracts all subjects have in common; changes of structures with high interindividual variability and gray matter changes associated with CH are not detected by this technique.

In conclusion, we were able to detect multiple brain areas with altered white matter microstructure in patients with episodic CH. These lesions were mainly evident in cortical and subcortical regions that are involved in nociceptive processes in CH. Additionally, we found structural changes in regions contributing to the olfactory, central sympathetic and trigemino-sensory system. Further studies with larger patient populations are necessary to confirm these results and to determine the role of our observed changes in the pathophysiology of CH.

STATEMENT OF AUTHORSHIP

Category 1

(a) Conception and Design

Michael Teepker; Katja Menzler; Susanne Knake; Marcus Belke; Veit Mylius; Wolfgang H. Oertel; Felix Rosenow; Johannes T. Heverhagen; Maximilian Voelker

(b) Acquisition of Data

Michael Teepker; Katja Menzler; Susanne Knake; Marcus Belke; Veit Mylius; Wolfgang H. Oertel; Felix Rosenow; Johannes T. Heverhagen; Maximilian Voelker

(c) Analysis and Interpretation of Data

Michael Teepker; Katja Menzler; Susanne Knake; Marcus Belke; Veit Mylius; Wolfgang H. Oertel; Felix Rosenow; Johannes T. Heverhagen; Maximilian Voelker

Category 2**(a) Drafting the Article**

Michael Teepker; Katja Menzler; Susanne Knake; Marcus Belke; Veit Mylius; Wolfgang H. Oertel; Felix Rosenow; Johannes T. Heverhagen; Maximilian Voelker

(b) Revising It for Intellectual Content

Michael Teepker; Katja Menzler; Susanne Knake; Marcus Belke; Veit Mylius; Wolfgang H. Oertel; Felix Rosenow; Johannes T. Heverhagen; Maximilian Voelker

Category 3**(a) Final Approval of the Completed Article**

Michael Teepker; Katja Menzler; Susanne Knake; Marcus Belke; Veit Mylius; Wolfgang H. Oertel; Felix Rosenow; Johannes T. Heverhagen; Maximilian Voelker

REFERENCES

1. May A. Cluster headache: Pathogenesis, diagnosis, and management. *Lancet*. 2005;366:843-855.
2. Headache Classification Committee of the International Headache Society. The International Classification of the Headache Disorders, 2nd edition. *Cephalalgia*. 2004;24:1-160.
3. Fischera M, Marziniak M, Gralow I, et al. The incidence and prevalence of cluster headache: A meta-analysis of population-based studies. *Cephalalgia*. 2008;28:614-618.
4. May A, Bahra A, Buchel C, et al. Hypothalamic activation in cluster headache attacks. *Lancet*. 1998;352:275-278.
5. May A, Ashburner J, Buchel C, et al. Correlation between structural and functional changes in brain in an idiopathic headache syndrome. *Nat Med*. 1999;5:836-838.
6. Morelli N, Pesaresi I, Cafforio G, et al. Functional magnetic resonance imaging in episodic cluster headache. *J Headache Pain*. 2009;10:11-14.
7. Sprenger T, Boecker H, Tolle TR, et al. Specific hypothalamic activation during a spontaneous cluster headache attack. *Neurology*. 2004;62:516-517.
8. Salat DH, Greve DN, Pacheco JL, et al. Regional white matter volume differences in nondemented aging and Alzheimer's disease. *Neuroimage*. 2009;44:1247-1258.
9. Knake S, Salat DH, Halgren E, et al. Changes in white matter microstructure in patients with TLE and hippocampal sclerosis. *Epileptic Disord*. 2009;11:244-250.
10. Knake S, Belke M, Menzler K, et al. In vivo demonstration of microstructural brain pathology in progressive supranuclear palsy: A DTI study using TBSS. *Mov Disord*. 2010;15;25:1232-1238.
11. Deppe M, Kellinghaus C, Duning T, et al. Nerve fiber impairment of anterior thalamocortical circuitry in juvenile myoclonic epilepsy. *Neurology*. 2008;71:1981-1985.
12. Jenkinson M, Bannister P, Brady M, et al. Improved optimization for the robust and accurate linear registration and motion correction of brain images. *Neuroimage*. 2002;17:825-841.
13. Basser PJ, Mattiello J, LeBihan D. Estimation of the effective self-diffusion tensor from the NMR spin echo. *J Magn Reson B*. 1994;103:247-254.
14. Basser PJ, Pierpaoli C. Microstructural and physiological features of tissues elucidated by quantitative-diffusion-tensor MRI. *J Magn Reson B*. 1996;111:209-219.
15. Smith SM, Jenkinson M, Johansen-Berg H, et al. Tract-based spatial statistics: Voxelwise analysis of multi-subject diffusion data. *Neuroimage*. 2006;31:1487-1505.
16. Smith SM, Jenkinson M, Woolrich MW, et al. Advances in functional and structural MR image analysis and implementation as FSL. *Neuroimage*. 2004;23(Suppl. 1):S208-S219.
17. Andersson JLR, Jenkinson M, Smith S. Non-linear registration, aka Spatial normalisation. 2007. FMRIB technical report TR07JA2 from <http://www.fmrib.ox.ac.uk/analysis/techrep>
18. Rueckert D, Sonoda LI, Hayes C, et al. Nonrigid registration using free-form deformations: Application to breast MR images. *IEEE Trans Med Imaging*. 1999;18:712-721.

19. Nichols TE, Holmes AP. Nonparametric permutation tests for functional neuroimaging: A primer with examples. *Hum Brain Mapp.* 2002;15:1-25.
20. Leone M, Bussone G. Pathophysiology of trigeminal autonomic cephalalgias. *Lancet Neurol.* 2009;8:755-764.
21. Sprenger T, Ruether KV, Boecker H, et al. Altered metabolism in frontal brain circuits in cluster headache. *Cephalalgia.* 2007;27:1033-1042.
22. Valet M, Sprenger T, Boecker H, et al. Distraction modulates connectivity of the cingulo-frontal cortex and the midbrain during pain—an fMRI analysis. *Pain.* 2004;109:399-408.
23. Bingel U, Lorenz J, Schoell E, et al. Mechanisms of placebo analgesia: rACC recruitment of a subcortical antinociceptive network. *Pain.* 2006;120:8-15.
24. Morris JS, Frith CD, Perrett DI, et al. A differential neural response in the human amygdala to fearful and happy facial expressions. *Nature.* 1996;383:812-815.
25. Parkin AJ. Human memory: The hippocampus is the key. *Curr Biol.* 1996;6:1583-1585.
26. Portas CM, Rees G, Howseman AM, et al. A specific role for the thalamus in mediating the interaction of attention and arousal in humans. *J Neurosci.* 1998;18:8979-8989.
27. Toni I, Krams M, Turner R, et al. The time course of changes during motor sequence learning: A whole-brain fMRI study. *Neuroimage.* 1998;8:50-61.
28. Bingel U, Quante M, Knab R, et al. Subcortical structures involved in pain processing: Evidence from single-trial fMRI. *Pain.* 2002;99:313-321.
29. Goadsby PJ, Edvinsson L. Human in vivo evidence for trigeminovascular activation in cluster headache. Neuropeptide changes and effects of acute attacks therapies. *Brain.* 1994;117(Pt 3):427-434.
30. Boivie J. Central pain in the face and head. *Handb Clin Neurol.* 2010;97:693-701.
31. Ordás CM, Cuadrado ML, Simal P, et al. Wallenberg's syndrome and symptomatic trigeminal neuralgia. *J Headache Pain.* 2011;12:377-380.
32. Warren HG, Kotsenas AL, Czervionke LF. Trigeminal and concurrent glossopharyngeal neuralgia secondary to lateral medullary infarction. *AJNR Am J Neuroradiol.* 2006;27:705-707.
33. Fang J, Jin Z, Wang Y, et al. The salient characteristics of the central effects of acupuncture needling: Limbic-paralimbic-neocortical network modulation. *Hum Brain Mapp.* 2009;30:1196-1206.
34. Peled S, Gudbjartsson H, Westin CF, et al. Magnetic resonance imaging shows orientation and asymmetry of white matter fiber tracts. *Brain Res.* 1998;780:27-33.
35. Song S, Sun S, Ramsbottom MJ, et al. Demyelination revealed through MRI as increased radial (but unchanged axial) diffusion of water. *Neuroimage.* 2002;17:1429-1436.
36. Song S, Sun S, Ju W, et al. Diffusion tensor imaging detects and differentiates axon and myelin degeneration in mouse optic nerve after retinal ischemia. *Neuroimage.* 2003;20:1714-1722.
37. Song S, Yoshino J, Le TQ, et al. Demyelination increases radial diffusivity in corpus callosum of mouse brain. *Neuroimage.* 2005;26:132-140.
38. Glenn OA, Henry RG, Berman JI, et al. DTI-based three-dimensional tractography detects differences in the pyramidal tracts of infants and children with congenital hemiparesis. *J Magn Reson Imaging.* 2003;18:641-648.
39. Beaulieu C, Allen PS. Determinants of anisotropic water diffusion in nerves. *Magn Reson Med.* 1994;31:394-400.
40. Menzler K, Belke M, Wehrmann E, et al. Men and women are different: Diffusion tensor imaging reveals sexual dimorphism in the microstructure of the thalamus, corpus callosum and cingulum. *Neuroimage.* 2011;54:2557-2562.
41. Schmitz N, Admiraal-Behloul F, Arkink EB, et al. Attack frequency and disease duration as indicators for brain damage in migraine. *Headache.* 2008;48:1044-1055.